Digital Signal Processing to Enhance Oceanographic Observations

TODD D. MUDGE AND ROLF G. LUECK

School of Earth and Ocean Sciences, University of Victoria, Victoria, British Columbia, Canada

(Manuscript received 7 June 1993, in final form 6 October 1993)

ABSTRACT

Quantization noise, the difference between a continuous physical signal and its discrete integer approximation, is an unavoidable consequence of data sampling. The problem is particularly acute for oceanographic data because these signals are usually red while the quantization noise is white, and this spectral mismatch limits our ability to detect short-term (high-frequency) fluctuations. A method of preemphasis and deconvolution is presented that reduces quantization noise and increases the resolution of short-term fluctuations by a factor of several hundred without any reduction in the full-scale range of the measurements. Examples are presented of a 12-bit thermometer with a range of −5° to 35°C and a resolution of 60 μ°C, and a 14-bit pressure gauge with a range of 600 db and a resolution of 1×10^{-4} db.

The preemphasis consists of summing a signal and its scaled time derivative before sampling. The enhanced version of the signal is recovered by convolving the preemphasized signal with a discrete single-pole low-pass filter with a time constant determined by the scale factor applied to the derivative. Alternatively, the signal and its derivative can be sampled separately and then combined in the discrete domain before deconvolution.

1. Introduction

Oceanic signals, like most natural processes, are essentially red; most of their energy is in the lower frequencies. The signal-to-noise ratio of measurements is usually poor at higher frequencies making it difficult to resolve small and short-term variations. The main source of noise in well-designed measurement systems is the conversion of the signal from the continuous domain into discrete integer samples, that is, the analog-to-digital (A/D) conversion. The difference between the continuous signal and its discrete approximation is called the quantization error and this noise is approximately white; it has the same energy density at all frequencies. At high frequencies the quantization noise dominates the measured signal.

The importance of preemphasizing the higher frequencies of a signal before it is recorded is well established for the continuous domain; the audio recording industry long ago established standards for phonographs and tapes. The playback process includes a deconvolution of the preemphasis to reproduce the original signal. The "recording and play-back process" for sampled data is similar except that the deconvolution must be discrete. We will demonstrate a method of preemphasis that consists of summing a signal and its scaled time derivative in the continuous domain before sampling (Fig. 1). Alternatively, one can sample the signal and its scaled derivative separately and then sum these in the discrete domain prior to deconvolution. An enhanced version of the original signal is retrieved by a numerically efficient discrete deconvolution. We applied this technique to two instruments: (i) a 14-bit pressure measurement system that resolved fluctuations of 10^{-4} db (1 db = 10^4 Pa) while maintaining a measurement range of 0–600 db, and (ii) a 12-bit thermometer that resolved 20 μ°C within its measurement range of −5° to 35°C. The sampling of a signal and its scaled derivative is standard practice in microstructure measurements and is easily implemented in any system where the sampled signal is an analog voltage—Sea-Bird Electronics has been producing such instruments for a number of years. Our deconvolution technique can also be applied directly to other signal enhancements such as matching thermometers and conductivity sensors on a CTD (Ochoa 1989) where it provides better phase fidelity.

The next section describes our technique in continuous time and frequency space. Section 3 introduces the z and bilinear transform, which provides a realization of the required deconvolution in the discrete (digital computer) domain. The technique is applied to observations of pressure in section 4. It is also applied to thermometry in section 5 where we show that it provides sufficient resolution to estimate Thorpe scales in the abyssal oceans, making it possible to estimate eddy diffusivity without measuring the rate of dissipation of kinetic energy. Section 6 shows how the technique is applied to CTD data, and the scope and limitations of the technique are discussed in section 7.

Corresponding author address: Dr. Rolf G. Lueck, School of Earth and Ocean Sciences, University of Victoria, P.O. Box 1700, Victoria, B.C., V8W 2Y2 Canada.

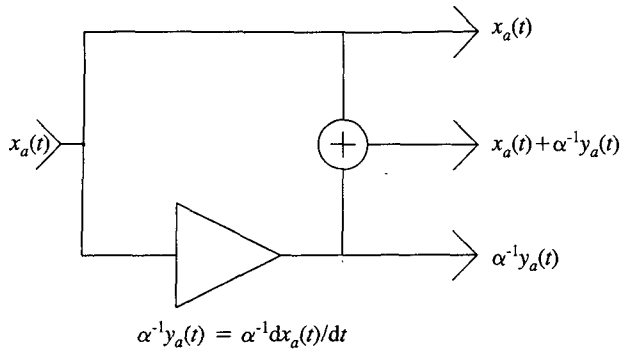

FIG. 1. Conceptual diagram for the production of a signal and its derivative prior to sampling by an A/D converter. Outputs can be either the signal and its derivative separately (upper and lower tracks) or a sum of a signal and its derivative (central track). The gain of the differentiator is α^{-1}.

2. The signal and its derivative

Let $x_a(t)$ and its scaled first derivative $y_a(t) = \alpha^{-1}dx_a(t)/dt$ be analog (continuous time domain) signals that are sampled separately (Fig. 1) to produce the discrete series

$$x_d(t) = x_a(t) + w(t), \tag{1}$$

and

$$y_d(t) = y_a(t) + v(t) = \frac{1}{\alpha}\frac{dx_a(t)}{dt} + v(t), \tag{2}$$

evaluated at $t = nT_s$, where T_s is the time between samples, n is the integer index of the samples, α^{-1} is the gain of the differentiator, and w and v are the quantization noise for the signal and its scaled derivative, respectively. We will consider w and v to be independent white noise sequences with bandwidths equal to the Nyquist frequency $F_n = \Omega_n/2\pi = (2T_s)^{-1}$ and variances of $\sigma^2 = \Delta^2/12$, where Δ is the bit size of the A/D converter (Proakis and Manolakis 1988). If the sampled data are not aliased, then we can consider x_d and y_d to be continuous functions for the purposes of this section.

The preemphasized signal $c(t)$ is obtained by summing the sampled signal $x_d(t)$ with the sampled derivative $\alpha y_d(t)$ such that

$$c(t) = x_d(t) + \frac{\alpha}{\Omega_c}y_d(t)$$

$$= \left[x_a(t) + \frac{1}{\Omega_c}\frac{dx_a(t)}{dt}\right] + \left(w + \frac{\alpha}{\Omega_c}v\right), \tag{3}$$

where the scaling factor Ω_c (required for dimensional consistency and denoted the cutoff frequency for reasons that will become clear later) is any real positive constant. The crucial point is that the derivative is created before sampling. The Fourier transform of this preemphasized signal (3) is

$$C(\Omega) = \left(1 + \frac{i\Omega}{\Omega_c}\right)X_a(\Omega) + W + \frac{\alpha}{\Omega_c}V, \tag{4}$$

where Ω is the angular frequency, X_a, W, and V are the Fourier transforms of x_a, w, and v, respectively, and we have used the property of differentiation; that is, $Y_a(\Omega) = i\Omega\alpha^{-1}X_a(\Omega)$.

The spectrum of the preemphasized signal $c(t)$ is

$$\Phi_c(\Omega) = \left(1 + \frac{\Omega^2}{\Omega_c^2}\right)\Phi_x(\Omega) + \left(1 + \frac{\alpha^2}{\Omega_c^2}\right)\Phi_w(\Omega), \tag{5}$$

where Φ_x and $\Phi_w = \sigma^2/\Omega_n$ are the spectra of $x_a(t)$ and the quantization noise, respectively. The first term on the right-hand side (rhs) of (5) is related to the signal of interest. For frequencies that are small compared to the cutoff frequency, ($\Omega \ll \Omega_c$), the signal portion of the spectrum comes predominantly from the sampling of x_a, while for $\Omega \gg \Omega_c$, it stems from the sampling of its scaled derivative y_a. The second term on the rhs of (5) is the noise spectrum and, compared to standard sampling (no preemphasis), it is larger by a factor of $1 + (\alpha/\Omega_c)^2$.

The enhanced version of the original signal, $x_e(t)$, is obtained by convolving (3) with a single-pole, low-pass filter having a transfer function $H_a(\Omega) = [1 + (i\Omega/\Omega_c)]^{-1}$; that is,

$$X_e(\Omega) = C(\Omega)H_a(\Omega)$$

$$= X_a(\Omega) + \frac{1}{1 + (i\Omega/\Omega_c)}\left(W + \frac{\alpha}{\Omega_c}V\right), \tag{6}$$

where Ω_c can now be interpreted as the half-power cutoff frequency of H_a. The enhanced signal is the original analog signal $x_a(t)$ plus low-pass-filtered white noise with the spectrum

$$\Phi_e(\Omega) = \frac{1 + (\alpha^2/\Omega_c^2)}{1 + (\Omega^2/\Omega_c^2)}\Phi_w. \tag{7}$$

The noise spectrum for standard sampling is Φ_w. Compared to standard sampling, the noise spectrum of the enhanced signal (7) is larger by a factor of $1 + (\alpha/\Omega_c)^2$ at low frequencies ($\Omega \ll \Omega_c$). Later, we will show that this factor is of order unity when α and Ω_c are optimized. Such a modest increase in noise at low frequencies is acceptable because the signal is red. For high frequencies, $\Omega \gg \Omega_c$, the noise spectrum is reduced by a factor of order $(\Omega/\alpha)^2$, a large reduction placed where it is needed the most.

The variance of the quantization noise in the enhanced signal is

$$\sigma_e^2 = \int_0^{\Omega_n}\Phi_e(\Omega)d\Omega, \tag{8}$$

where Ω_n is the Nyquist frequency (rad s^{-1}). For any choice of the cutoff frequency small compared to the Nyquist frequency, $\Omega_c \ll \Omega_n$, the variance of the quantization noise in the enhanced signal is

$$\sigma_e^2 = \frac{\pi}{2\Omega_c\Omega_n}(\Omega_c^2 + \alpha^2)\sigma^2, \quad (9)$$

while the variance without preemphasis is

$$\sigma^2 = \Omega_n\Phi_w = \frac{\Delta^2}{12}. \quad (10)$$

Thus, the overall improvement provided by the preemphasis is the ratio of these variances; that is,

$$\frac{\sigma_e^2}{\sigma^2} = \frac{\pi}{2\Omega_c\Omega_n}(\Omega_c^2 + \alpha^2). \quad (11)$$

One objective criterion for choosing the cutoff frequency Ω_c (3) is the reduction of overall variance (11), which takes its minimum of $\pi\Omega_c/\Omega_n$ at $\Omega_c = \alpha$. The cutoff frequency can also be chosen on the basis of how it blends a signal with its derivative. The cutoff frequency Ω_c should be small compared to the frequency at which the spectrum of x_d becomes dominated by quantization noise; otherwise, no benefit is realized by summing the signal with its scaled derivative. Alternatively, one could decide upon the highest frequency of interest and then choose Ω_c so that it boosts the spectrum of the derivative signal above the noise spectrum of x_d for all frequencies of interest. This last method is utilized for a pressure signal in section 4.

An alternate strategy is to sum the continuous signals $x_a(t)$ and $\alpha^{-1}y_a(t)$ into a single signal (Fig. 1). The enhanced signal is recovered by choosing $\Omega_c = \alpha$. This method is utilized for thermometry in section 5. As there is only one source of quantization noise, the noise spectrum (7), variance (9), and overall improvement (11) are reduced by 2.

The implementation of the deconvolution (6) is trivial in the continuous domain; it requires one resistor, one capacitor, and one operational amplifier. In the next section we show how this deconvolution is achieved efficiently with a numerical algorithm in the discrete domain.

3. The z and bilinear transform

The z transform of a discrete series is

$$X(z) = \sum_{n=-\infty}^{\infty} x(n)z^{-n}, \quad (12)$$

where z is a complex variable (Proakis and Manolakis 1988). When z is evaluated on the unit circle, $z = \exp(i\pi\omega/\Omega_n)$, the z transform is the discrete Fourier transform of a doubly infinite series and provides the frequency domain representation of operations in the discrete time domain. Note that because of the interval of (12), the frequency ω of the discrete signal $x(n)$ is a continuous function over the principle interval $\pm\Omega_n$. The z transform shares many of the properties of the Fourier transform (linearity, convolution, etc.) and has the useful property that the transform of a delayed series $x(n - n_o)$ is simply

$$\sum_{n=-\infty}^{\infty} x(n - n_o)z^{-n} = z^{-n_o}X(z). \quad (13)$$

There are a number of methods for mapping transfer functions of the continuous domain into the discrete domain and, among these, the bilinear transform

$$i\Omega = 4F_n\left(\frac{z-1}{z+1}\right) \quad (14)$$

(Proakis and Manolakis 1988) is both simple and effective.

From (3), the preemphasized discrete series is

$$c(n) = x(n) + \frac{\alpha}{\Omega_c}y(n), \quad n = 1, 2, 3\cdots, \quad (15)$$

and, from (4), we want a filter with the transfer function

$$H(z) \approx \left[1 + i\left(\frac{\omega}{\Omega_c}\right)\right]^{-1}, \quad z = \exp\left(\frac{i\pi\omega}{\Omega_n}\right) \quad (16)$$

to approximate the continuous domain deconvolution (6). Equating the continuous domain frequency Ω with the discrete domain frequency ω and using the bilinear transform (14) gives

$$H(z) = \frac{a(1 + z^{-1})}{1 - bz^{-1}}, \quad (17)$$

where

$$a = \left(\frac{4F_n}{\Omega_c} + 1\right)^{-1}, \quad b = 1 - 2a. \quad (18)$$

The z transform of the enhanced data series, $x_e(n)$, is then given by

$$X_e(z) = H(z)C(z)$$

$$X_e(z) - bX_e(z)z^{-1} = a[C(z) + C(z)z^{-1}]$$

and, by exploiting the shift property (13), the time domain convolution is

$$x_e(n) = bx_e(n - 1) + a[c(n) + c(n - 1)] \quad n = 1, 2, 3\cdots. \quad (19)$$

The enhanced series is computed recursively using one past output, $x_e(n - 1)$, and the present and one past input, $c(n)$ and $c(n - 1)$, of the preemphasized signal. The algorithm requires initial unknown values $x_e(0)$ and $c(0)$, but the choice of $x_e(0) = c(0) = c(1)$ is reasonable and virtually eliminates start-up transients.

Our algorithm is summarized as follows:

(i) sample the signal and its derivative separately,
(ii) chose the cutoff frequency Ω_c,

(iii) combine these two signals using (15), and
(iv) filter this combination using (19).

Compared to standard sampling, this enhanced signal costs only three additions and three multiplications per data point [one each for step (iii) and another two each for step (iv)]. If the signal and its derivative are not sampled separately but are combined in the continuous domain before sampling, then step (iii) is not needed but the cutoff frequency is then forced to equal the inverse gain of the differentiator; that is, $\Omega_c = \alpha$.

The drawback of the bilinear transform is that it nonlinearly maps frequencies from the continuous domain into the discrete domain. Evaluating z on the unit circle and using (14) shows that the mapping is

$$\frac{\omega}{4F_n} = \tan^{-1}\left(\frac{\Omega}{4F_n}\right). \qquad (20)$$

This mapping is linear only for frequencies that are small compared to the Nyquist frequency and it warps the higher frequencies by equating infinite frequency in the continuous domain with the Nyquist frequency in the discrete domain. At low frequencies, $F \leq F_n/10$, the frequencies from the two domains agree within better than 1% (Antoniou 1979) and they accord within 10% for $F \leq F_n/3$. For the low-pass filter of (19), this warping produces a greater than desired attenuation at high frequencies—some detail at the shortest timescales is smoothed. This is not a serious limitation for the following two reasons: (i) data are usually oversampled to avoid aliasing, and (ii) if spectra are the objective of the measurements, these can be corrected using (20) to within a few percent of the Nyquist frequency.

4. Pressure enhancement

The technique of preemphasis outlined above was applied to pressure data collected with the towed, microstructure instrument HOTDAD (Horizontal Ocean Data Acquisition Device) during the C-SALT (Caribbean-Sheets and Layers Transect) experiment (Lueck 1987; Fleury and Lueck 1991). Pressure and its derivative were sampled into two channels at 64 Hz and quantized into 14-bit integers. The bit resolution of the pressure record was 0.04 db and insufficient for plotting hydrographic parameters against depth without some smoothing of the pressure record.

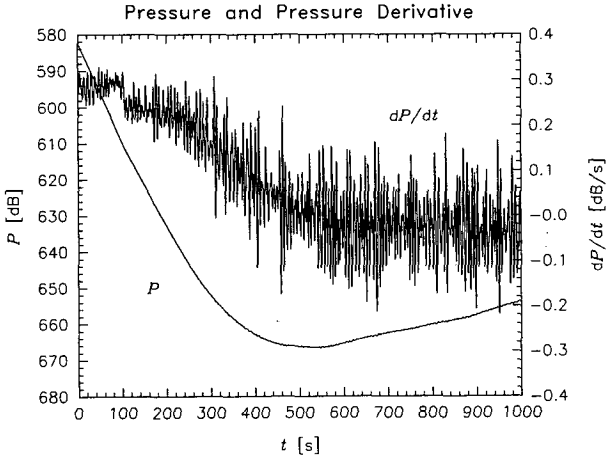

FIG. 2. Pressure and its derivative reported by the microstructure instrument HOTDAD during the C-SALT experiment.

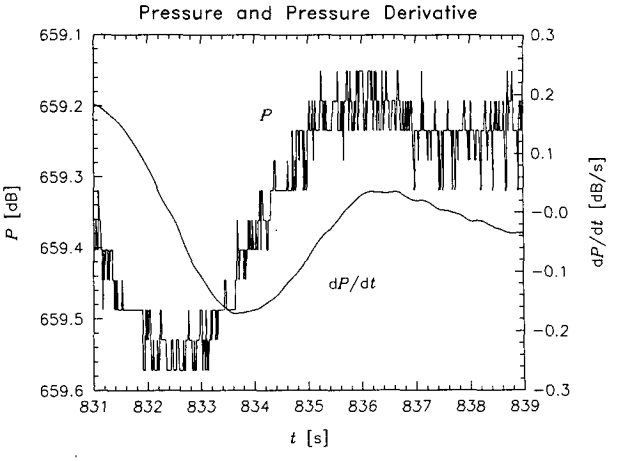

FIG. 3. A short segment of data shown in Fig. 2.

Variations of the pressure signal over short timescales are negligible compared to changes over long time scales (Fig. 2), while changes of the pressure derivative over large and small timescales have similar magnitudes; hence, the pressure record is red and may improve with preemphasis. This difference in character of the two series at short timescales is even more apparent in an 8-s segment of data (Fig. 3). At short time scales the pressure record is dominated by quantization noise while none is evident in the samples of pressure derivative. The spectra of the two signals reflects this difference in temporal character (Fig. 4). The spectrum of pressure flattens above 1 Hz reaching the quantization noise asymptotically; hence, the pressure record has useful information only below approximately 0.5 Hz. In contrast, the spectrum of pressure derivative flattens above 8 Hz. This corner frequency exceeds the response of the analog electronics and probably the response of the sensor; thus, useful information for frequencies above 0.5 Hz is found only in the derivative record, while both records provide data for frequencies smaller than 0.5 Hz. Unfortunately, there is a large and narrow 4-Hz signal in both records due to a problem with the power supply. This noise limits the range of interest to only 3.5 Hz (circles in Fig. 4), so we attempted to improve the pressure measurements up to this frequency.

The main concern with preemphasis is choosing an appropriate value for the cutoff frequency Ω_c. The ratio $\alpha = 1/200$ is known from the calibration of the elec-

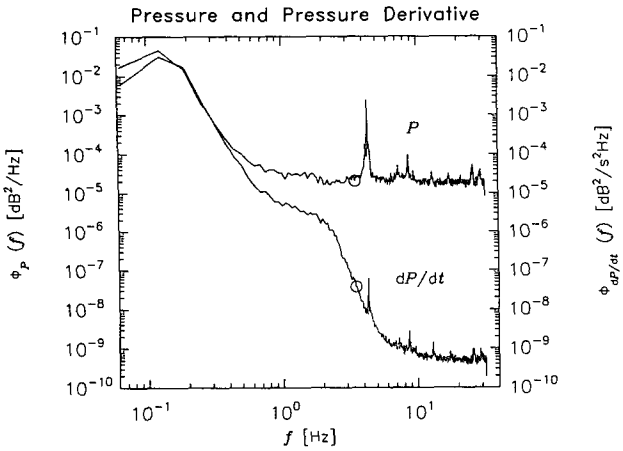

FIG. 4. The spectra of pressure and its derivative for the data shown in Fig. 2. The circles are positioned at 3.5 Hz.

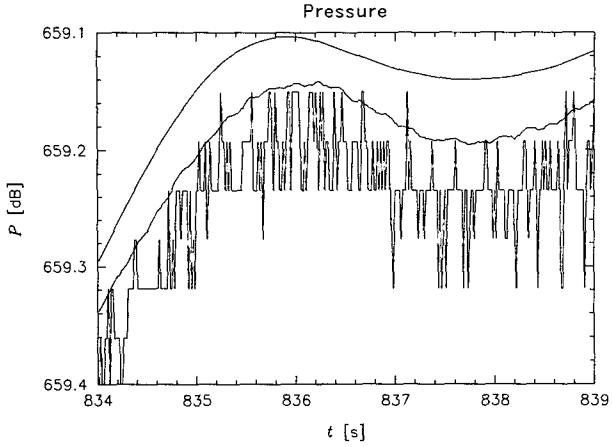

FIG. 5. The original pressure record (lowest curve), the enhanced pressure using $\Omega_c = 1/21$ (upper curve intentionally offset for clarity), and the original pressure smoothed with a 1-s running mean (central curve and also offset).

tronics and is reflected by the square root of the ratio of the spectra at high frequencies (where they are flat). As shown by (11), the choice of $\Omega_c = \alpha$ gives the lowest *total* variance; however, we are not interested in frequencies above 3.5 Hz and satisfactory results will be obtained for $\Omega_c > \alpha$. Our criterion is that at 3.5 Hz the spectrum of the derivative divided by Ω_c exceeds the spectrum of pressure [see (3) and (15)] and this criterion is met by taking $\Omega_c \leq 1/20$. We chose $\Omega_c = 1/21$, which implies that the enhanced signal will have a signal-to-noise ratio of unity at 3.5 Hz and a progressively higher ratio at lower frequencies. The improvement provided in the time domain by preemphasis (Fig. 5) is considerable—bit noise is not detectable even in a plot spanning 0.2 db. Our choice of Ω_c gives favorable signal-to-noise ratios for all frequencies smaller than 3.5 Hz and so bit noise should be negligible for time scales longer than approximately $[(2\pi)3.5\ \text{Hz}]^{-1} = 0.045$ s. Spectra of the original and enhanced pressure records (Fig. 6) also demonstrate the benefits of preemphasis—the band of useful signal has been increased by a factor of approximately 10.

The noise in the enhanced signal is now frequency dependent (7), making it difficult to give an objective value for the resolution of this signal. We used two methods to quantify the improvement provided by preemphasis—the ratio of the spectra of the original and enhanced signals at the highest frequency of interest (3.5 Hz), and the reduction in overall noise variance (11). The ratio of the spectra at 3.5 Hz is 90 900; hence, $\Delta_o/\Delta_e = (90\ 900)^{1/2} \approx 300$, where $\Delta_o = 0.04$ db is the bit size of the original pressure record. Thus, $\Delta_e = 1.3 \times 10^{-3}$ db is the "bit" resolution of the enhanced pressure. The observed improvement of 300 is close to the theoretical prediction (7) of 470 for $\alpha^{-1} = 200$ and $\Omega_c = 21$, and the additional noise at low frequencies ($\Omega \ll \Omega_c$) is negligible because $\Omega_c \gg \alpha$ (7). For the highest frequency of interest, this improvement is equivalent to having used an A/D converter with an additional 9 bits, that is, a 23-bit converter; however, this analogy does not apply at lower frequencies, because the noise spectrum of a converter is white while the noise spectrum of the enhanced signal (7) is red. The noise spectrum of the enhanced signal (straight line in Fig. 6) has been computed on the assumption that the noise spectrum of the original pressure record is white and equal to the flat portion of the spectrum at high frequencies. The ratio of signal + noise-to-noise takes a minimum of approximately 2 near 3.5 Hz as

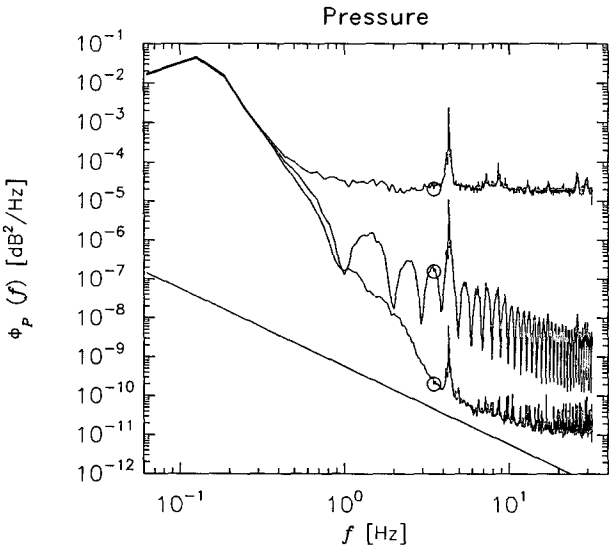

FIG. 6. Spectrum of the pressure data shown in Fig. 2; original data (upper curve); 1-s smoothed data (middle curve); enhanced pressure record (lower curve). The nearly straight and diagonal line is the noise spectrum of the enhanced pressure. The circles are positioned at 3.5 Hz.

expected, but it does not asymptotically reach unity at higher frequencies, which at first may seem surprising. The spectra were computed with single-precision floating point numbers (24-bit mantissa) and the asymptotic behavior of the spectrum of the enhanced signal merely reflects numerical round-off errors, even though the filtering was performed with double-precision arithmetic; thus, this technique taxes the limits of single-precision computations. Finally, the overall reduction in variance (11), which includes frequencies well beyond our interest, is a factor of 2.6×10^3, and the square root of this, namely, 50, is the overall reduction in bit size. Thus, the overall reduction in quantization error is a factor of 50, noise has been reduced by a factor of 300 at the highest frequency of interest, and the useful bandwidth has been increased by a factor of approximately 10.

Sampling and other noise in a signal is more traditionally reduced by smoothing such as a running mean. To contrast the technique of preemphasis against simple smoothing, we applied a running mean filter to the pressure record that was symmetric about its midpoint. A running mean filter will reduce high-frequency noise seen in a signal but, unfortunately, it will also attenuate low frequencies. Clearly, some smoothing is justified because signals above 3.5 Hz are beyond our interest and, because the Nyquist frequency is 32 Hz, only one in $32/3.5 \approx 9$ points is important. For the pressure data, a running mean filter of 1-s length (64 points) gives a good balance between the most attenuation of noise and the least decrease of real (low-frequency) signal. Although smoothing provides a significant improvement (Fig. 5), the bit noise is still clearly visible. The spectrum of filtered pressure (Fig. 6) is biased by the noise spectrum and remains above the spectrum of enhanced pressure for all frequencies above 0.5 Hz. This limits the useful band of smoothed data to below 0.5 Hz. The strength of preemphasis is that it smooths the pressure record by *adding* information from the derivative record, which has a high signal-to-noise ratio. Filtering of the pressure record never adds new information; instead, it removes information, less being lost for sharper spectral cutoffs.

5. Temperature enhancement

a. Motivation

A major goal of oceanic fine and microstructure measurements is the estimation of eddy diffusivity. Direct measurements of shear at dissipation scales using airfoil probes (Osborn and Crawford 1980) is currently the most popular technique for estimating the eddy diffusivity using

$$K_\rho = \frac{\Gamma \epsilon}{N^2} \tag{21}$$

(Osborn 1980), where Γ is the mixing efficiency and considered to be in the range of 0.05 to 0.2 (Gargett 1984), ϵ is the rate of dissipation of kinetic energy, and N is the buoyancy frequency. The resolution of ϵ with present techniques is generally considered to be 1×10^{-10} W kg^{-1} (Moum and Lueck 1985), although recent profilers may be capable of 1×10^{-11} W kg^{-1} (J. Toole 1993, personal communication). Given the small buoyancy frequency of the abyssal oceans (Table 1), the more conservative resolution implies that the eddy diffusivity must exceed 10^{-5} m^2 s^{-1} at 1000 m and 10^{-3} m^2 s^{-1} at 4000 m to be detectable by dissipation measurements. Estimates of eddy diffusivity in the abyssal oceans are very uncertain and are thought to lie in the range of 10^{-6}–10^{-4} m^2 s^{-1} (Garrett 1991). The dissipation technique may thus be marginal.

An alternative technique for estimating diffusivity is measuring the Thorpe scale l_T, the root-mean-square (rms) vertical distance of particle displacement due to turbulence. The Thorpe scale is usually computed by resorting a vertical temperature profile into a monotonic profile where temperature decreases with increasing depths (Dillon 1982). For meaningful results, the water column must be free from salinity compensated temperature inversions and the temperature–salinity relationship must be reasonably smooth. Producing temperature profiles that resolve the displacement of water over a Thorpe scale, when the mean temperature gradient is of order 1 m°C m^{-1}, is a major difficulty with this method. The temperature gradients in Table 1 have been estimated using

$$T_z = 1.5N^2\left(\frac{g}{\rho}\frac{\partial \rho}{\partial T}\right)^{-1},$$

where g is the acceleration of gravity, ρ is the density, and the factor of 1.5 accounts for the contribution of salinity to density in the deep Pacific. If we take T' as the difference in the actual temperature from the sorted monotonic temperature, then

$$\langle T'^2 \rangle^{1/2} \approx l_T T_z, \tag{22}$$

where the angle brackets indicate a suitable depth average, l_T is the Thorpe scale, and T_z is the mean vertical gradient. Because (22) gives the expected rms temperature fluctuation, a conservative estimate of the smallest fluctuations that must be resolved is about a tenth of $l_T T_z$. The actual resolution required will depend upon the statistical distribution of T' and may be much

TABLE 1. Pacific Ocean abyssal buoyancy frequency after Munk (1966), and vertical temperature gradients.

D (m)	1000	2000	3000	4000
$10^3 N$ (rad s^{-1})	2.6	1.5	0.94	0.49
$10^3 T_z$ (°C m^{-1})	3.7	1.1	0.4	0.1

TABLE 2. Thorpe scales in the abyssal Pacific Ocean and a conservative estimate of the temperature resolution ($0.1 l_T T_z$) required to detect these scales for three hypothetical eddy diffusivities.

K_ρ ($m^2 s^{-1}$)	1 km	2 km	3 km	4 km
10^{-4}	0.44 m/160 μ°C	0.58 m/64 μ°C	0.73 m/29 μ°C	1.0 m/10 μ°C
10^{-5}	0.14 m/52 μ°C	0.18 m/20 μ°C	0.23 m/92 μ°C	0.32 m/3.2 μ°C
10^{-6}	0.044 m/16 μ°C	0.058 m/6.4 μ°C	0.073 m/2.9 μ°C	0.10 m/1.0 μ°C

less demanding than $0.1 l_T T_z$ if deep mixing (like its shallower counterpart) is intermittent.

With strong averaging the Thorpe scale is approximately the same as the Ozmidov scale l_o (Crawford 1986), and using (21) we can take

$$l_T \approx l_o = \left(\frac{\epsilon}{N^3}\right)^{1/2} = \left(\frac{K_\rho}{\Gamma N}\right)^{1/2} \qquad (23)$$

(Gargett and Holloway 1984). The Thorpe scale for depths of 1000–4000 is given for three hypothetical diffusivities in Table 2 along with a conservative estimate of the temperature resolution required to detect these Thorpe scales. The required temperature resolution ranges from 1 to 160 μ°C. Is the measurement of Thorpe scales a feasible technique for estimating diffusivity in the abyssal oceans?

b. *High-resolution temperature*

In June of 1992, vertical profiles of microstructure shear and temperature were taken around Cobb Seamount (46°45'N, 130°48'W) with the profiler FLY II (Dewey et al. 1987). Shear measured by an airfoil probe and preemphasized temperature detected with an FP-07 thermistor were sampled at 274 Hz by a 12-bit A/D convertor. FLY II supports only two fast channels, so temperature and its derivative were combined in the continuous domain before sampling (Fig. 1). The analog electronics were set so that temperatures from −5° to 35°C covered the full range of the converter and the gain of the differentiator was set to α^{-1} = 0.50 s. This forced the choice of $\Omega_c = \alpha = 2.0$ rad s^{-1} in the discrete deconvolution to recover the enhanced temperature signal. The data are dominated by the derivative signal for frequencies larger than about 1/3 Hz. The chosen temperature range of −5° to 35°C provided adequate head room for the derivative signal.

A profile of sampled signal (temperature plus its scaled derivative) expressed in units of the least significant bit (or integer counts) is shown in Fig. 7 along with the deconvolved and enhanced temperature (°C). The bit resolution of the temperature without preemphasis would have been $\Delta_T = 40/2^{12} \approx 9.5$ m°C. The airfoil shear signal (not shown) indicates that the region between 180 and 225 m was turbulent. At these depths the mean temperature gradient was less than 1 m°C m^{-1} (Fig. 8) and comparable to gradients in the abyssal oceans. Clearly, the resolution of the enhanced temperature surpasses considerably the 9.5-m°C limit of the original combined signal.

To estimate the improvement provided by preemphasis, we have examined a very quiescent section of data from a deep profile taken more than 10 km from the seamount (Fig. 9). A wave of about 15 s (approx-

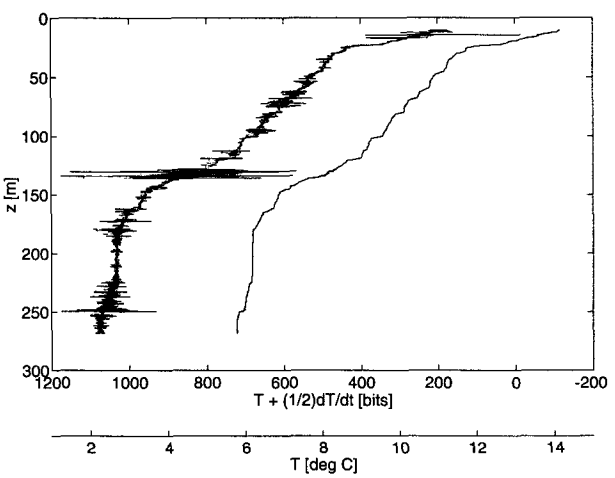

FIG. 7. The original preemphasized temperature record taken with FLY II (left curve) expressed as integers and enhanced temperature in physical units.

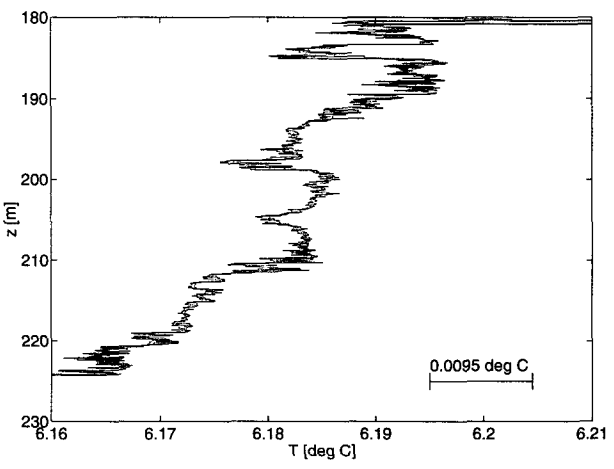

FIG. 8. A 50-m segment of data shown in Fig. 7. This section is turbulent and has a mean vertical gradient of less than 1 m°C m^{-1}. The solid horizontal line indicates the size of a bit prior to preemphasis.

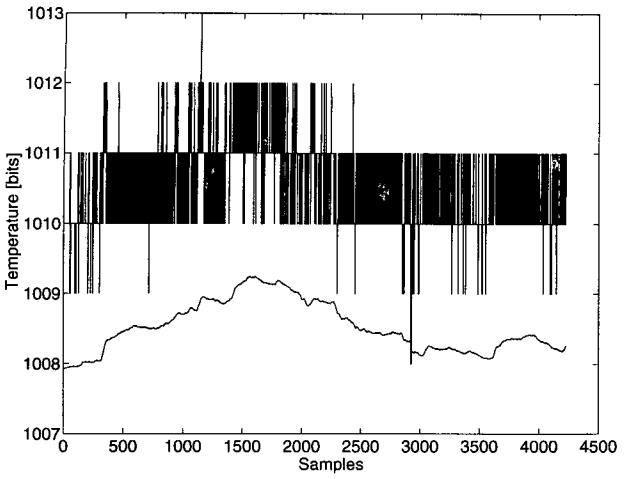

FIG. 9. A 15-s section of very quiescent data in integer units; preemphasized signal (upper curve) and enhanced signal (lower curve) lowered by two counts for clarity.

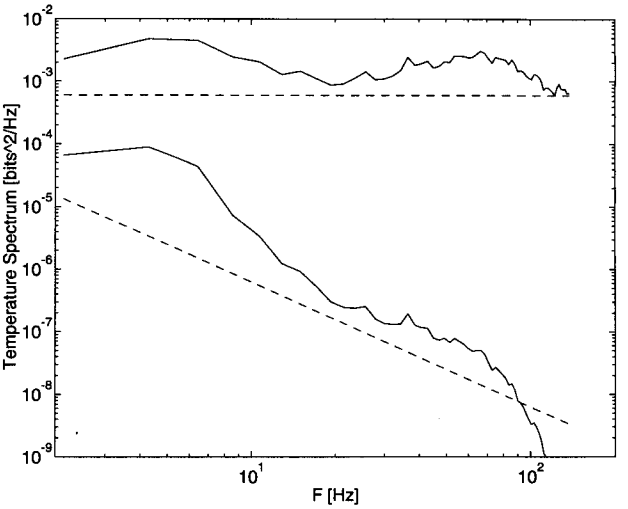

FIG. 10. Spectra of data in Fig. 9; preemphasized signal (upper solid curve) and its noise level (upper dashed line); enhanced signal (lower solid curve) and its noise spectrum (sloping dashed curve).

imately 4000 samples) is evident in the preemphasized signal but all shorter term data are masked by bit noise. We have expressed the enhanced signal in terms of original bit size (9.5 m°C) to facilitate comparisons. The amplitude of the short-term fluctuations is about 0.01 bit. The spectrum of the preemphasized and enhanced signals are shown in Fig. 10 along with the noise spectrum for an ideal A/D converter and the noise spectrum after ideal low-pass filtering. The preemphasized signal is very close to the theoretical noise level. Comparing the enhanced spectrum against the noise spectrum of the preemphasized signal shows that no signal would have been detected above 1 Hz without preemphasis. The highest frequency to which the data can be interpreted as temperature is about 50 Hz. Above 50 Hz there is considerable smoothing by the analog electronics, and the thermistor attenuates signals above 20 Hz. From the ratio of the noise spectra at 50 Hz we estimate a hypothetical bit size of 0.006 or an improvement of about 160 for our choice of differentiator gain. The overall variance is reduced by 16^2 and, if we ignore data above 50 Hz, the variance is diminished by 10^2. The enhanced signal drops below the theoretical noise above 100 Hz because of frequency warping (section 3).

Preemphasis has raised the resolution from 9.5 m°C to 60 μ°C at 50 Hz. The choice of a 12-bit A/D converter was not under the control of the authors. If we extrapolate the resolution obtained with a 12-bit converter to a 16-bit unit, then 4-μ°C resolution is achievable with preemphasis and Thorpe scales may be measurable in the abyssal oceans. Johnson noise is about 2 μ°C (Gregg et al. 1978).

The local displacement of the water parcels was greatest in the region of 180–225 m, and the rms Thorpe scale was clearly resolved, being about 7 m in this region (Fig. 11). Although the mean gradients are similar to abyssal gradients, the Thorpe scale for mixing around Cobb seamount is about a factor of 10 larger than expected for abyssal conditions—the diffusivity implied by a 7-m Thorpe scale is 10^{-2} m^2 s^{-1}. The successful resolution of Thorpe scales under such strong mixing does not by itself guarantee equally successful results in the abyssal oceans but it provides grounds for optimism.

It is worth noting that the technique of combining a signal with its scaled derivative is used in the SBE 7-02 microstructure conductivity probe and the SBE 8-02 microstructure thermometer manufactured by Sea-Bird Electronics Incorporated. For these systems, α^{-1}

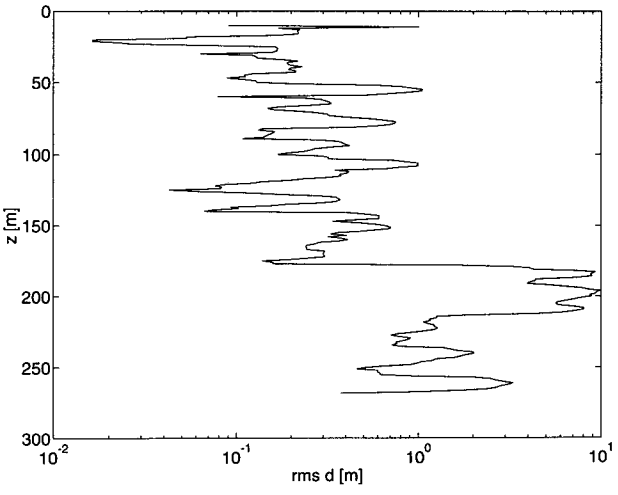

FIG. 11. Profile of rms displacement (Thorpe scale) smoothed with a 5-m running average.

is set to approximately $5/\pi$. The deconvolution discussed here may be helpful to users of these instruments.

6. CTD data processing

Our technique is largely a method of discrete signal processing that can also be applied to other types of data processing problems such as matching signals from thermometers and conductivity sensors on CTDs. Bray (1987) and Ochoa (1989) used two methods of decreasing salinity spiking that are amenable to the technique presented here; both attempted to reduce or remove the relative lag of a platinum resistance thermometer (PRT) with respect to a conductivity probe. We will bypass all discussion of the appropriateness of the various models of sensor response that are used to match CTD sensors and, instead, merely demonstrate how these continuous domain models can be implemented in the discrete domain.

In Bray (1987), temperature signals from a PRT and a fast-response thermistor (FRT) on a Neil Brown Mark III CTD were combined to produce a temperature record with the long-term precision of the PRT and the short-term resolution of the FRT that, by itself, exhibits considerable drift on long time scales. Using a running mean to filter the data, she produced an enhanced temperature record by adding the high-passed FRT signal to the low-passed PRT signal; that is,

$$T_e(t) = \langle T_{\mathrm{PRT}}(t)\rangle + [T_{\mathrm{FRT}}(t) - \langle T_{\mathrm{FRT}}(t)\rangle], \quad (24)$$

where the angle brackets indicate a running mean. The best results were obtained for a running mean of length $\tau = 60$ s covering approximately 2000 data samples. As indicated in section 4, running means provide inefficient smoothing with large spectral side lobes. The main advantage of a running mean is that it can be made numerically efficient by taking advantage of its equal weighting. A well-written algorithm requires only two additions and one multiplication per data point; however, for nonuniform weighting, the number of additions and multiplications is approximately the width of the smoothing window.

If, instead of a running mean, we choose a Butterworth low-pass filter, then (24) is equivalent to

$$T_e(\Omega) = \frac{1}{1 + (i\Omega/\Omega_c)} T_{\mathrm{PRT}}(\Omega) + \frac{i\Omega/\Omega_c}{1 + (i\Omega/\Omega_c)} T_{\mathrm{FRT}}(\Omega), \quad (25)$$

which reduces to

$$T_e(\Omega) = \frac{1}{1 + (i\Omega/\Omega_c)} \left[T_{\mathrm{PRT}}(\Omega) + \frac{i\Omega}{\Omega_c} T_{\mathrm{FRT}}(\Omega) \right]. \quad (26)$$

Equation (26) is similar to the technique of preemphasis. Filtering the FRT and PRT signals as in (24) is equivalent to combining the temperature of the PRT with the temperature derivative of the FRT and then low-pass filtering this combination to produce an enhanced signal. Using the bilinear transformation, (26) becomes

$$T_e(n) = bT_e(n-1) + a[T_{\mathrm{PRT}}(n) + T_{\mathrm{PRT}}(n-1)] + c[T_{\mathrm{FRT}}(n) - T_{\mathrm{FRT}}(n-1)], \quad (27)$$

where a and b are given in (18) and $c = 1 - a$. A Butterworth filter with a cutoff frequency of $\Omega_c = \pi(1.1\tau)^{-1}$ gives a smoothing similar to a running average of width τ. The enhancement algorithm of (27) requires four additions and three multiplications per data point or, through the simple relationship between a, b, and c, seven additions and one multiplication. Thus, (27) is less efficient than a running mean but its initial transient response can be minimized through a proper choice of initial values while a running average has a transient response lasting $\tau/2$ and, being causal, (27) can be implemented in real time.

Ochoa (1989) took a somewhat different approach to reducing salinity spiking caused by the mismatch in response times of Neil Brown CTD sensors. His method is meant for the Smart CTD, which does not carry an FRT and, thus, Bray's technique is not applicable. The phase lag of the PRT signal was reduced by filtering its signal backwards using a digital filter with a transfer function similar to that of the PRT. The transfer function of the PRT was taken to be characterized by

$$\tau \frac{dT_{\mathrm{PRT}}}{dt} + T_{\mathrm{PRT}} = T_0, \quad (28)$$

where T_0 is the actual temperature. In fact, (28) is another way of expressing the first-order, low-pass, Butterworth filter, where T_{PRT} is its output, T_0 its input, and $\Omega_c = \tau^{-1}$. The discrete approximation of (28) used by Ochoa was

$$T_{\mathrm{PRT}}(n) = (1 - \beta)T_0(n) + \beta T_{\mathrm{PRT}}(n-1), \quad (29)$$

where $\beta = \exp(-T_s/\tau)$ and T_s is the time between samples. At first glance, (29) appears to be a reasonable approximation of (28) and may have first been used for CTD data processing by Fofonoff et al. (1974); however, (29) is flawed in that its asymptotic phase at high frequencies tends to 0 while the phase of (28) tends to $-\pi/2$; that is, (29) is one-half sample time out of step with (28). This mismatch is easily seen by comparing the Fourier transform of (28) against the z transform of (29) evaluated on the unit circle. Phase is much more important than amplitude when matching signals, and this asymptotic phase mismatch may be responsible for some of the difficulties reported by Ochoa. For example, he obtained favorable results for a Mark III CTD with $T_s \ll \tau$ or equivalently $\Omega_n \gg \Omega_c$,

while the reduction in spikes was less satisfactory for the Smart CTD with $T_s \approx \tau$. An alternative discrete approximation to (28) with good phase fidelity is obtained by taking the Fourier transform of (28), applying the bilinear transform (14), and then using the shift property (13) to produce

$$T_{\mathrm{PRT}}(n) = a[T_0 + T_0(n-1)] + bT_{\mathrm{PRT}}(n-1), \tag{30}$$

where, as in (18),

$$a = \frac{1}{1 + 4F_n\tau} = \frac{1}{1 + (2\tau/T_s)}, \quad b = 1 - 2a. \tag{31}$$

The main difference between (30) and (29) is the additional term $T_0(n-1)$, which centers the input T_0 midway between n and $n-1$ and, thereby, imparts an asymptotic phase shift of $-\pi/2$ at the Nyquist frequency. The phases of (28), (29), and (30) are compared in Fig. 12 for $\tau = 0.3$ s and the two values of T_s examined by Ochoa. Since only frequencies up to approximately 1 Hz are important, we see that in the first case (Fig. 12a), having $T_s = 0.04$ s, that the phase error of Ochoa's deconvolution (29) is less than 10°; however, for the second case (Fig. 12b), having $T_s = 0.2$ s, the phase error of (29) reaches 50° at 1 Hz. For both cases, the phase error of the bilinear approximation (30) is small at all frequencies.

7. Discussion and conclusions

a. Discussion

Although preemphasis can dramatically increase the resolution of a signal, its application should be considered carefully. It is very appropriate for signals that are red because it whitens the signal before quantization. Signals that are already relatively white may be better served by simple smoothing. The technique requires some a priori information about the expected range of a signal and the magnitude of its maximum rate of change so that the gain of the differentiator, α^{-1}, can be chosen to cover as fully as possible the span of the A/D converter. The derivative signal will be saturated and, hence, useless if the differentiator gain is too large. On the other hand, the derivative signal will have too little boost at higher frequency and remain close to the quantization noise if the gain is set too low. The sensors themselves must be fast enough that the higher-frequency information contains useful data. Profiling instruments are ideal candidates for preemphasis; however, "high frequency" is a relative term. The technique is also useful for moored and stationary sensors provided that the signal is red.

The cutoff frequency Ω_c must also be chosen with some care. If the signal is added to its scaled derivative in the continuous domain prior to sampling, then Ω_c must equal α; there is no other choice! The choice of cutoff frequency is not constrained if summing occurs in the discrete domain after sampling. However, poor results will follow for cutoff frequencies that are much smaller and much larger than α. If Ω_c is very large, the derivative samples contribute very little to the preemphasized signal [see Eq. (3)], and the benefits are small. If the cutoff frequency is very small, the preemphasized signal is strongly dominated by the derivative samples, which are unreliable at very low frequencies. The spectrum of the derivative signal, being proportional to the signal spectrum times frequency squared, must ultimately fall below the quantization noise spectrum as $\Omega \to 0$; thus, low-frequency information is compromised. The enhanced signal will also suffer from numerical instability when Ω_c is excessively small. From (17) and (18) it is clear that the deconvolution coefficient b approaches unity as $\Omega_c \to 0$ and b eventually

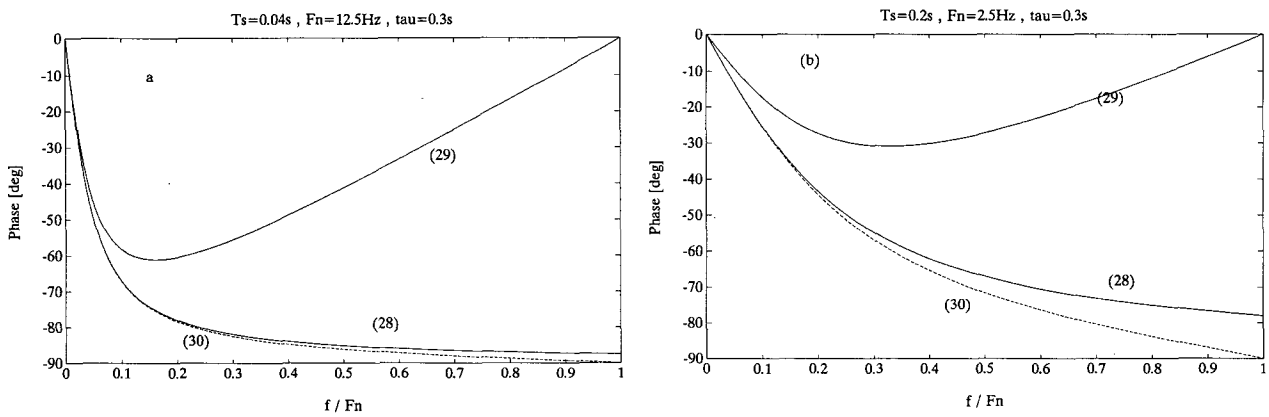

FIG. 12. Phase versus frequency normalized by the Nyquist frequency for the first-order linear thermometer of Eq. (28), the discrete approximation of Ochoa Eq. (29), and the bilinear approximation Eq. (30) for two cases considered by Ochoa (1989); (a) $T_s = 0.04$ s corresponding to a Mark III CTD; (b) $T_s = 0.2$ s corresponding to a Smart CTD.

becomes indistinguishable from exactly one for a computer with finite word length.

Preemphasis does not increase the accuracy of sampled measurements; it increases the high-frequency or short-term resolution of a signal by decreasing the quantization error. Accuracy is a matter of calibration and stability. The International Temperature Scale of 1990 (Bedford 1990, chapter 2) is defined only to 0.001°C. Small temperature differences, hence relative temperature, can be interpolated beyond this limit of 0.001°C. The maximum time scale over which the extra resolution is meaningful will depend on the instrumentation and how it is used. For example, most thermometers are sensitive to pressure and some portion of the enhanced signal may reflect variations of pressure rather than temperature or, through self-heating, reflect variations in flow past the sensor. Likewise, the electronics supporting a sensor may induce variations of the measured signal due to temporal drifts and environmental changes around the circuitry. Noise and other spurious signals in the continuous domain (i.e., before sampling) are treated as real signals by the technique of preemphasis. The prudent user must evaluate the significance of these and other effects. As a rule, the longer the time scale over which minute but real variations of a signal are to be detected, the more significant will be the contribution of secondary effects.

A significant practical consideration is signal offset. For Ω_c small compared to unity, the derivative signal is amplified considerably (3 and 15) and small offsets produced by analog electronics may add a significant bias to the enhanced signal. Bias in the derivative samples can be minimized by (i) defining the mean derivative to be the difference between the last and first sample of the (undifferentiated) signal divided by the time between these samples and then (ii) adjusting the derivative record by a constant to make its mean equal to the above-defined mean. Due to bias, potential numerical instability, and excessive low-frequency noise, we were reluctant to make Ω_c smaller than necessary in the preemphasis of the pressure record (section 4).

A signal compression of almost a factor of 2 is obtained by summing the signal with its scaled derivative before sampling. For example, if an m-bit system has been set up so that the signal and its derivative *each* fully span the range of an A/D converter, then a sum of these signals requires a converter with $m + 1$ bits. The saving is $(m + 1)/2m$. Summing the signal and its derivative before sampling also appears to reduce the quantization noise of the enhanced signal by a factor of 2 compared to sampling the signal and its derivative separately. However, the amplitude of the signal and its derivative must be reduced by a factor of 2 for the sum to fit into the range of the converter. The variance of the enhanced signal is then smaller by a factor of 4 and the final ratio of noise-to-signal variance is larger by a factor of 2; hence, there is no real improvement in reducing quantization noise by summing the signal and its derivative before sampling rather than summing after sampling.

b. *Conclusions*

It is possible to significantly reduce quantization noise by preemphasizing data before sampling or, alternatively, by sampling both the signal and its derivative. With both methods, the preemphasized data is a linear combination of a signal and its time derivative. A numerically efficient deconvolution of the data returns the original signal plus low-pass-filtered white noise. Examples were provided for pressure and temperature measurements. Compared to conventional sampling, signal resolution was improved by a factor of 300 and 160 at the highest frequency of interest for pressure and temperature, respectively. The overall noise variance was reduced by a factor of 2600 and 256 for pressure and temperature, respectively. The method of preemphasis is easily implemented in all measurement systems where the signal is an analog voltage. The method may permit measurements, such as Thorpe scales in the abyssal oceans, that hitherto were considered impractical.

Acknowledgments. We received very helpful comments from L. Maas, C. Garrett, J. Toole, and the referees. We are particularly indebted to W. Crawford for the use of FLY-II. This work was supported by the Office of Naval Research under Grant N00014-89-J1607 and by a grant from NSERC/DFO. TDM was partially supported by an Atlantic Accord Career Development Award.

REFERENCES

Antoniou, A., 1979: *Digital Filters: Analysis and Design.* McGraw-Hill, 524 pp.

Bedford, R. E., 1990: Physical principles. *Thermal Sensors,* W. Gopel, J. Hesse and J. N. Zemel, Eds., VCH, 412 pp.

Bray, N. A., 1987: Salinity calculation techniques for separately digitized fast response and platinum resistance CTD temperature sensors. *Deep-Sea Res.,* **34,** 627–632.

Crawford, W. R., 1986: A comparison of length scales and decay times of turbulence in stably stratified flows. *J. Phys. Oceanogr.,* **16,** 1847–1854.

Dewey, R. K., W. R. Crawford, A. E. Gargett, and N. S. Oakey, 1987: A microstructure instrument for profiling oceanic turbulence in coastal bottom boundary layers. *J. Atmos. Oceanic Technol.,* **4,** 288–297.

Dillon, T. M., 1982: Vertical overturns: A comparison of Thorpe and Ozmidov length scales. *J. Geophys. Res.,* **87,** 9601–9613.

Fleury, M., and R. G. Lueck, 1991: Fluxes across a thermohaline interface. *Deep-Sea Res.,* **38,** 745–769.

Fofonoff, N. P., S. P. Hayes, and R. C. Millard Jr., 1974: W.H.O.I/Brown CTD microprofiler: Methods of calibration and data handling. W.H.O.I. Tech. Rep. WHOI-74-89, 64 pp.

Gargett, A. E., 1984: Vertical eddy diffusivities in ocean interior. *J. Mar. Res.,* **42,** 359–393.

——, and G. Holloway, 1984: Dissipation and diffusion by internal wave breaking. *J. Mar. Res.,* **42,** 359–393.

Garrett, C. J. R., 1991: Marginal mixing theories. *Atmos.-Ocean,* **29,** 313–339.

Gregg, M. C., T. Meagher, A. Pederson, and E. Aagaard, 1978: Low noise temperature microstructure measurements with thermistors. *Deep-Sea Res.,* **25,** 843–856.

Lueck, R. G., 1987: Microstructure measurements in a thermohaline staircase. *Deep-Sea Res.,* **10,** 1677–1688.

Moum, J. N., and R. G. Lueck, 1985: Causes and implication of noise in oceanic dissipation measurements. *Deep-Sea Res.,* **32,** 379–390.

Munk, W. H., 1966: Abyssal recipes. *Deep-Sea Res.,* **13,** 707–730.

Ochoa, J., 1989: A practical determination of CTD resistance thermometer response time, and its use to correct salinity bias and spikes. *Deep-Sea Res.,* **36,** 139–148.

Osborn, T. R., 1980: Estimation of the local rate of diffusion from dissipation measurements. *J. Phys. Oceanogr.,* **4,** 109–115.

——, and W. R. Crawford, 1980: An airfoil probe for measuring turbulent velocity fluctuation in water. *Air–Sea Interaction: Instruments and Methods,* F. Dobson, L. Hase, and R. Davis, Eds., Plenum.

Proakis, J. G., and D. G. Manolakis, 1988: *Introduction to Digital Processing.* MacMillan Pub., 944 pp.